SANDIA REPORT

SAND96–0956 • UC–400
Unlimited Release
Printed April 1996

The Faradaic Efficiency of the Lithium - Thionyl Chloride Battery

S. N. Hoier, E. T. Eisenmann

Prepared by
Sandia National Laboratories
Albuquerque, New Mexico 87185 and Livermore, California 94550
for the United States Department of Energy
under Contract DE-AC04-94AL85000

Issued by Sandia National Laboratories, operated for the United States Department of Energy by Sandia Corporation.

Available to DOE and DOE contractors from
Office of Scientific and Technical Information
PO Box 62
Oak Ridge, TN 37831

Prices available from (615) 576-8401, FTS 626-8401

Available to the public from
National Technical Information Service
US Department of Commerce
5285 Port Royal Rd
Springfield, VA 22161

NTIS price codes
Printed copy: A03
Microfiche copy: A01

SAND96-0956
Unlimited Release
Printed April 1996

Distribution
Category UC-400

The Faradaic Efficiency of the Lithium - Thionyl Chloride Battery

S. N. Hoier and E. T. Eisenmann

Battery Research Department
Sandia National Laboratories
Albuquerque, NM 87185

Abstract

The efficiency of converting chemical energy into electrical energy has been studied for the case of D-size, low and medium rate lithium-thionyl chloride (Li/TC) cells, under DC and various pulsed loads. Microcalorimetric monitoring of the heat output during discharge allowed the direct measurement of the faradaic efficiency, and showed that self-discharge is far more pervasive than previously acknowledged by researchers and battery manufacturers. Evaluations of the cell dynamics prove that current load and temperature fluctuations combine to disrupt the lithium passivation and to greatly enhance self-discharge. Typical faradaic efficiencies for DC range from about 30% at low current density to 90% at moderate and 75 % at high current density. Pulsed current further depresses these efficiency levels, except at very low average current densities. The decreased faradaic efficiency of Li/TC batteries in certain pulse situations needs to be studied further to define the range of applications for which it can be successfully used.

Contents

Figures

The Faradaic Efficiency of the Lithium - Thionyl Chloride Battery

Introduction

Batteries are electrochemical energy converters that offer, under ideal conditions, 100% efficiency, as compared to Carnot-limited heat-engines with efficiencies of 50% or less. How close to ideal conditions Li/TC cells operate is a question, which has, in the pertinent literature, received less attention than it deserves, although self-discharge is a well recognized phenomenon for these devices. Self-discharge of Li/TC cells comes about because of the direct reaction of lithium with the solvent, according to

$$4\,Li + 2\,SOCl_2 \rightarrow 4\,LiCl + SO_2 + S \qquad (1)$$

Useful energy can only be extracted by means of the two separate reactions

$$Li \rightarrow Li^+ + e^- \text{ at the anode} \qquad (2)$$

$$\text{and } 4\,Li^+ + 4\,e^- + SOCl_2 \rightarrow 4\,LiCl + SO_2 + S \text{ at the cathode.} \qquad (3)$$

Accumulating LiCl at the lithium-electrolyte interface slows reaction (1) and has been referred to as passivation layer or solid electrolyte interface, SEI[1]. The SEI presumably is a pure ion conductor that blocks all charge transfer reactions, but allows Li^+ ions to freely migrate from the lithium metal surface into the liquid electrolyte. In actuality, the SEI cannot be as effective as claimed, since self-discharge leads to coarse-crystalline LiCl layers of many micrometers thickness[2,3], in a process that does not seem to be self-limiting. This contrasts with the much thinner passivation layers on aluminum, titanium or tantalum. The LiCl-buildup is reasonably blamed for the voltage delay, which manifests itself as an instantaneous collapse of the voltage at the start of current flow, with recovery usually occurring within seconds. This effect clearly shows that passage of current removes the passivation layer, which grows again after the current stops. In the absence of a passivation layer reaction (3) proceeds largely uninhibited, and a continuous load effectively keeps the passivation layer from forming. An issue of major significance is how intermittent loads affect the cumulative faradaic efficiency.

This report reviews literature data and presents new results from experiments in which the self-discharge of Li/TC cells is measured by microcalorimetry. P. Bro,[4] for example, describes calorimetric measurements of D cells and concludes that the heat effects were two to three times greater than should be expected on the basis of the Peltier effect. His data convert into faradaic efficiencies of 85 to 95 %, and show a decrease for increasing

current and temperature. Takeuchi, Meyer and Holmes[5] report on the capacity loss in low-rate lithium/bromine chloride thionyl chloride cells. Their data convert into faradaic efficiencies of 60 % at high, and 80% at low current density. Both datasets were measured with constant current, but specific interests in pulsed conditions made a new study necessary.

The present experimental evaluation started with the characterization of the microcalorimeter in terms of (1) transients in the operating temperature and (2) transients in the heat flow. Knowing the time constants of the instrument is important for the differentiation between system and specimen responses. With this approach it became apparent that not only current loads, but also temperature variations activate the lithium anode by destroying the passivation layer.

A secondary goal of the present study was to find an alternative to time consuming microcalorimetric tests. An attempt was made to calibrate complex impedance measurements against the calorimetric data, because impedance tests were thought to provide an easy way for collecting data on film formation and the co-dependent self-discharge. However, as the results will show, the correlation between cell impedance and self-discharge is complicated because the test interferes with the growth of the passivation layer. Eventually, microcalorimetric test series were determined to be the fastest, most reliable method to measure the faradaic efficiency of Li/TC cells for various load conditions.

Instrument Stabilization Rates

The calorimeters used in this study are of the heat conduction type, Micro-Therm Model 1701 by Hart Scientific, offering temperature stability of ±0.005 C and a heat flow detection range of 0 to 65 mW, at a resolution of approximately 1μW. The calibration procedure calls for two periods of controlled current through precision resistors in either of the two test cavities and stipulates 5.5 hours for stabilizing the instrument output. This time corresponds to 82.5 minutes per transient. Figure 1 shows the semilogarithmic plots of two calibration transients, one for an empty cavity and the second for an aluminum cylinder of the size of a D cell placed in the cavity. The reciprocal slopes of the least squares fitted lines represent the time constants of the transients and show that the empty cavity reaches 90% equilibration in about 11 minutes, while the aluminum cylinder takes about twice as long.

Much longer equilibration times apply to situations where the operating temperature of the microcalorimeter is readjusted. Although the temperature can be quickly raised with a built-in heater, many hours are needed for the heat flow detector to settle down. Figure 2 illustrates the responses for temperature adjustments from 5 to 10 C and back to 5 C. In fact, lines a and b show that the time constants for raising or lowering the temperature are essentially the same for up to 5 hours, about 10 hours/decade. At longer times, in the case of a temperature increase, the equilibration rate accelerates and steady state is reached

after about 8 hours. Lowering the operating temperature of the calorimeter exclusively relies on the refrigeration unit of the thermostat and the rate of equilibration remains constant. In either case, the temperature stabilizes long before the heat flow detector achieves a constant reading.

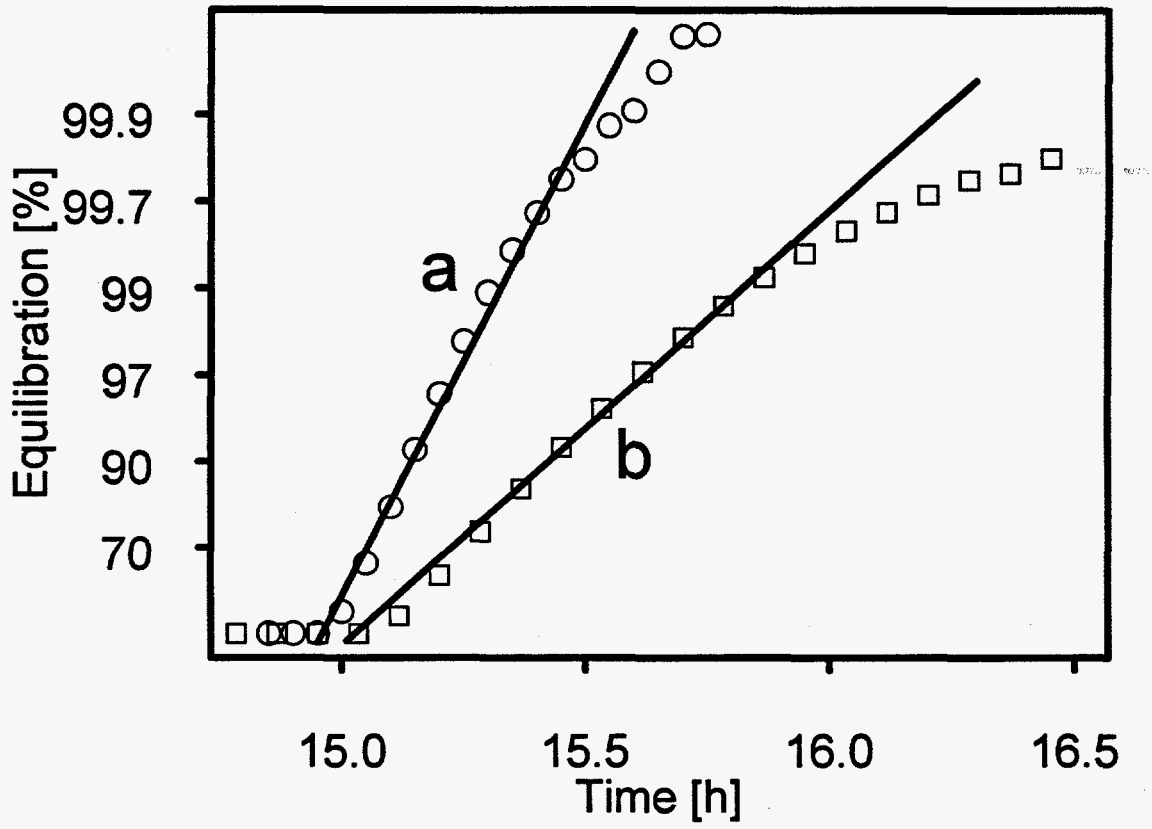

Figure 1: Normalized thermal transients of the microcalorimeter during calibration: (a) empty cavity; (b) D cell-sized aluminum cylinder in cavity. The reciprocal slopes of the regression lines represent time constants, which amount to (a): 0.184 hours/decade and (b): 0.398 hours/decade.

The performance of the microcalorimeter, as illustrated in Figures 1 and 2, can be characterized as follows:

1. The heat flow detector, which includes a bridge circuit, accurately responds to changes in heat flow if its range is not significantly exceeded, i.e. if the heat flow is not substantially above 65 mW. The rate of equilibration is then controlled by the heat capacity (or mass) occupying the test cavity, and by any transient heat sources, including chemical reactions.
2. If the heat flow is greater than 100 mW and the detector remains off-scale for an extended period of time, then balancing difficulties occur and the readings must be assumed to be false, even if the signal is back on scale. This is the case whenever the test temperature changes, a new specimen is placed in the test cavity or an excessively large burst of heat is generated in the cavity.

Kinetic studies of Li/TC cells need to consider this potentially sluggish response of the instrument so that the thermal effects of the battery will not be confused with the instrument response rate.

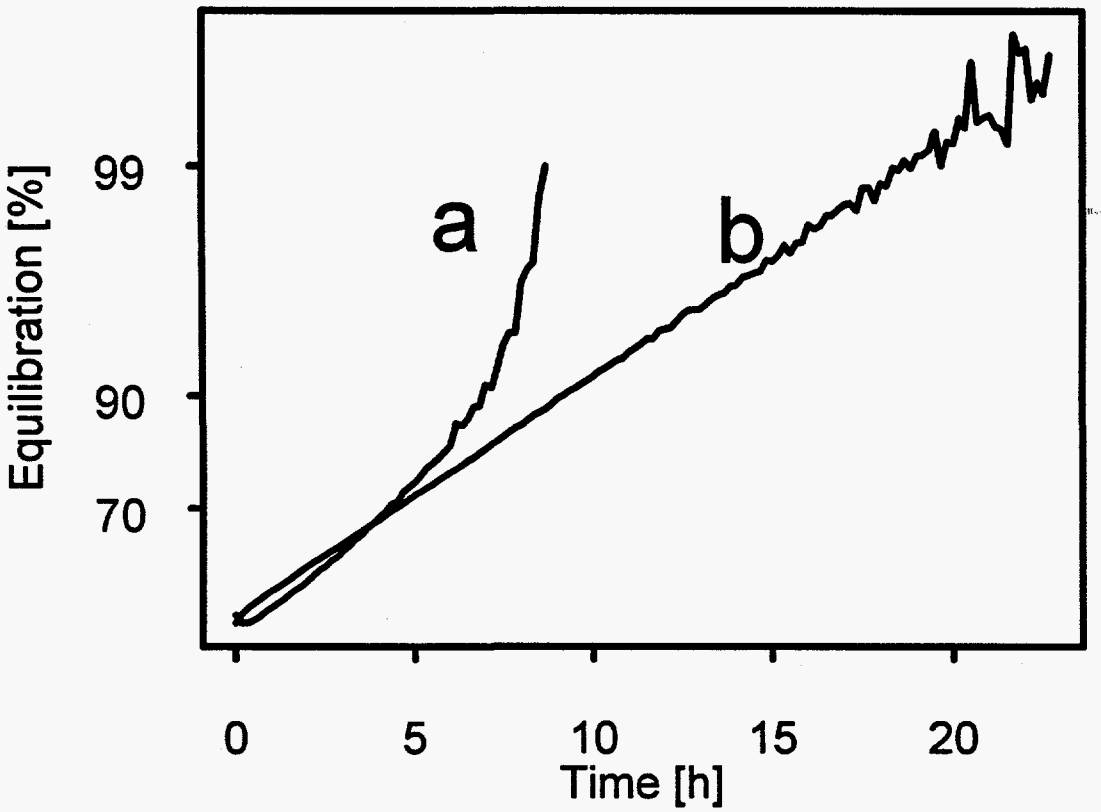

Figure 2: Thermal transients (with D cell-sized aluminum cylinder in cavity) of the microcalorimeter after adjustment of the operating temperature. (a): Heater assisted increase from 5 to 10 C. (b): Temperature decrease from 10 to 5 C. The initial slope for both lines corresponds to a time constant of about 9 hours/decade.

Effects of Temperature Transients on the Self-Discharge of Li/TC Cells

Figure 3 shows the typical response of the microcalorimeter if the test cavity contains a Li/TC D cell and the temperature is stepped from 5 and 10 and back to 5 C. As in Figure 2, the initial rate of equilibration is about 10 hours/decade, but the rapid rise in temperature now causes a slow-down in equilibration, while the slow rate of cooling accelerates it. These effects appear after the instrument effect is already 97 % complete and continue for more than 20 hours in the case of rising temperature. They are results of chemical processes in the cell and could be identified as such only after having characterized the instrument response.

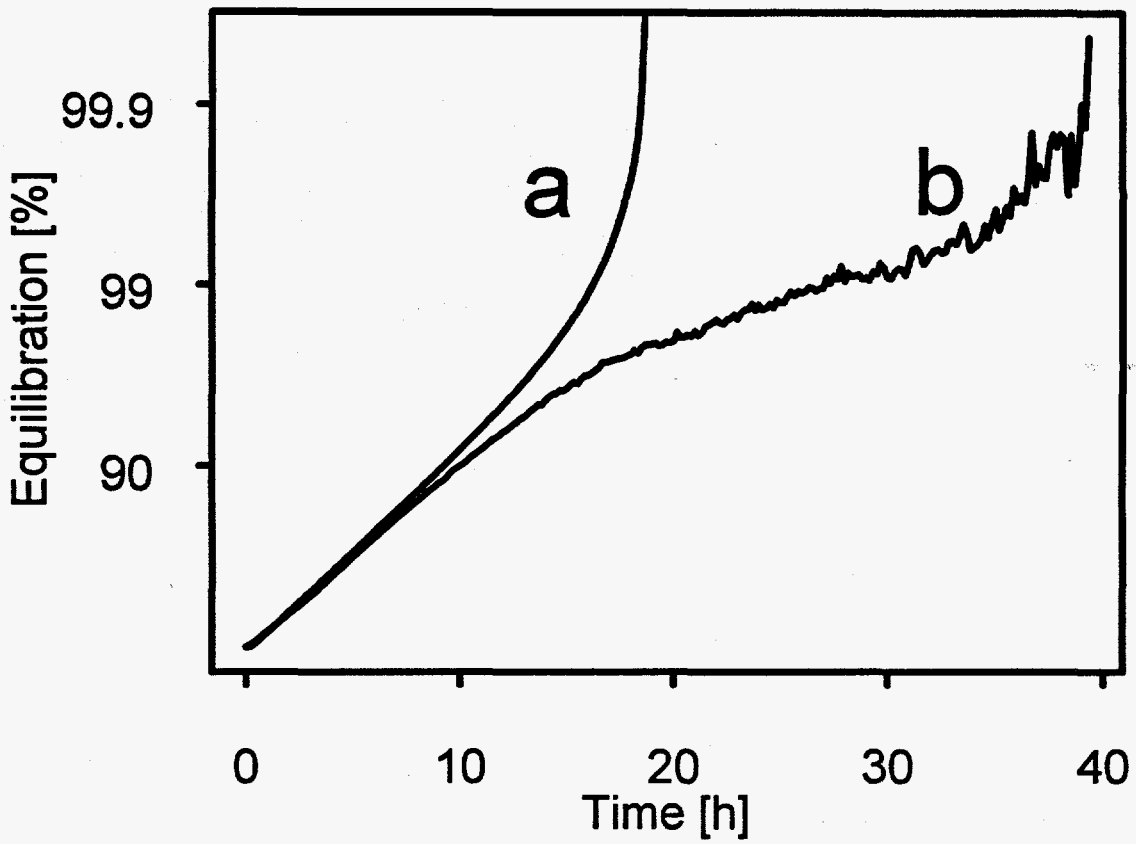

Figure 3: Thermal transients for Li/TC -cell in the cavity of the microcalorimeter after adjustment of the operating temperature. (a): Heater assisted increase from 5 to 10 C. (b): Temperature decrease from 10 to 5 C. The initial slopes equal those shown in Figure 2.

Measuring the heat output of a Li/TC cell is an in-situ way to determine its rate of self-discharge, and one may reasonably expect that higher temperature accelerates the process. However, the observed times for equilibration are contrary to what should be expected for a thermally activated process. In fact, reaction (1) most certainly is not thermally activated, but instead proceeds as fast as thionyl chloride can migrate to the lithium surface. Obviously, the key to the rate limitation of reaction (1) is the LiCl passivation layer, and the observed effects are consistent with thermal stresses that disrupt the integrity and the protective properties of the Li / LiCl interface layer. Rapid temperature changes generate higher stress levels and lead, therefore, to a more extensive break-down of the passivation layer and require more time for repassivation.

Other observations completely agree with this interpretation. For example, cells that can be assumed to be well passivated after being stored at -40 C for several month showed unexpected high rates of self-discharge in the 5 C microcalorimeter. Similarly, a cell whose self-discharge had substantially quieted down during an extended period in the microcalorimeter became highly active after a brief removal from the test chamber. These observations suggest that the passivation layer provides no permanent protection against self - discharge.

Impedance Measurements for Passivation Studies

Li/TC cells exhibit voltage delay at the start of a discharge and continue to self-discharge at a high rate and for many hours after the electrical discharge has ceased, as has been first reported by P. Bro.[4] This behavior is consistent with the break-down of the passivation layer during current flow and complements the thermal effects described above. However, these observations are inconsistent with the SEI concept, and there is a dearth of information about the extent of the de-passivation and the rate of re-passivation. Gaberscek[2] et al. measured the rise in cell impedance over time and showed in an Arrhenius plot that the interfacial resistance may change from less than 100 Ωcm^2 at 45 C to more than 10 $K\Omega cm^2$ at -55 C. This technique for assessing the passivation of the lithium electrode has been used by other investigators,[6] and has great appeal because of the potential for rapid data acquisition. All that seems necessary for instantaneous measurements of the self-discharge of Li/TC cells is to calibrate impedance data against microcalorimetric standards. According to this principle, cells were first thermally equilibrated in the microcalorimeter, then discharged through a 1.5 Ω resistor for 30 seconds. This caused the cell to become active and to exhibit a high rate of self-discharge that decreased with time. Impedance measurements over a frequency range from 10,000 to 10 Hz were made at 5 minute intervals at an amplitude of 5 mV. Figure 4 shows the results obtained for three test conditions with two cells and two temperatures. Admittance is shown on the abscissa, because the heat flow due to self-discharge is expected to be inversely proportional to the resistance of the passivation layer. Indeed, the data form an approximately linear pattern over three orders of magnitude on both axes.

However, there are some features for which an explanation is speculative. The distinctive change in slope at about 0.8 S is possibly attributable to the passivation layer changing from discontinuous to uniform, while the kinks in the 30 C response lines look like an instrument error, although none could be identified. Even more troubling was the observation that substantial currents, up to 60 mA at low frequency, passed through the cell under the influence of the 5 mV AC amplitude applied during the impedance test. This degree of cell polarization most certainly will affect the passivation layer, just as the 30 second discharge at the start of the experiment maximally activated the cell. Figure 5 shows the results of an experiment in which the heat flow from an active cell was read every 10 minutes, while impedance tests were repeated every 30 minutes. Each impedance measurement generates a spike in the heat flow because the 5 mV polarization activates the lithium surface. (Note: The periodicity of the spike amplitude is a harmonic that has its origin in the incomplete synchronization between the microcalorimetric and the impedance readings, which were taken by two computers). Figure 5 also illustrates that the heat flow levels off above 0.6 mW, which is a far higher level than would be observed if the cell remained undisturbed. Therefore, if impedance measurements are used to check the degree of passivation of a Li/TC cell, all possible precautions must be taken not to falsify the outcome of the test. For example, reducing the voltage amplitude and restricting the measurements to high frequencies will be prerequisites for making this test a viable procedure. For the remainder of the present investigation microcalorimetry was the exclusive method of data acquisition.

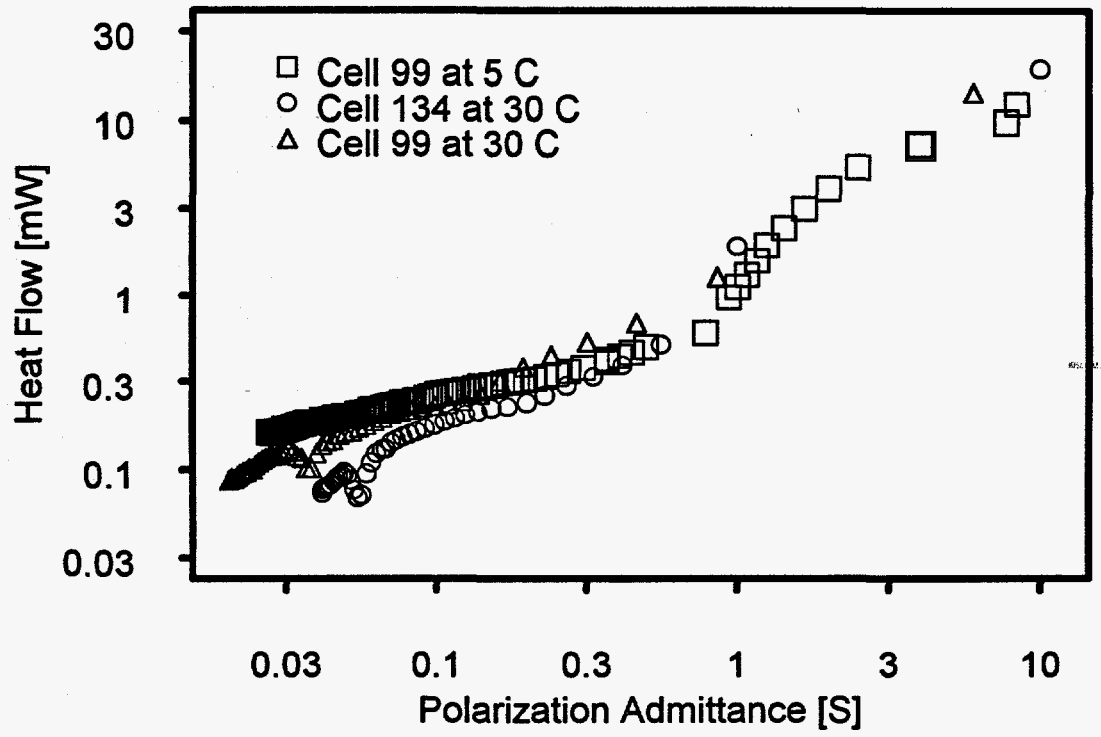

Figure 4: Heat flow versus admittance calibration.

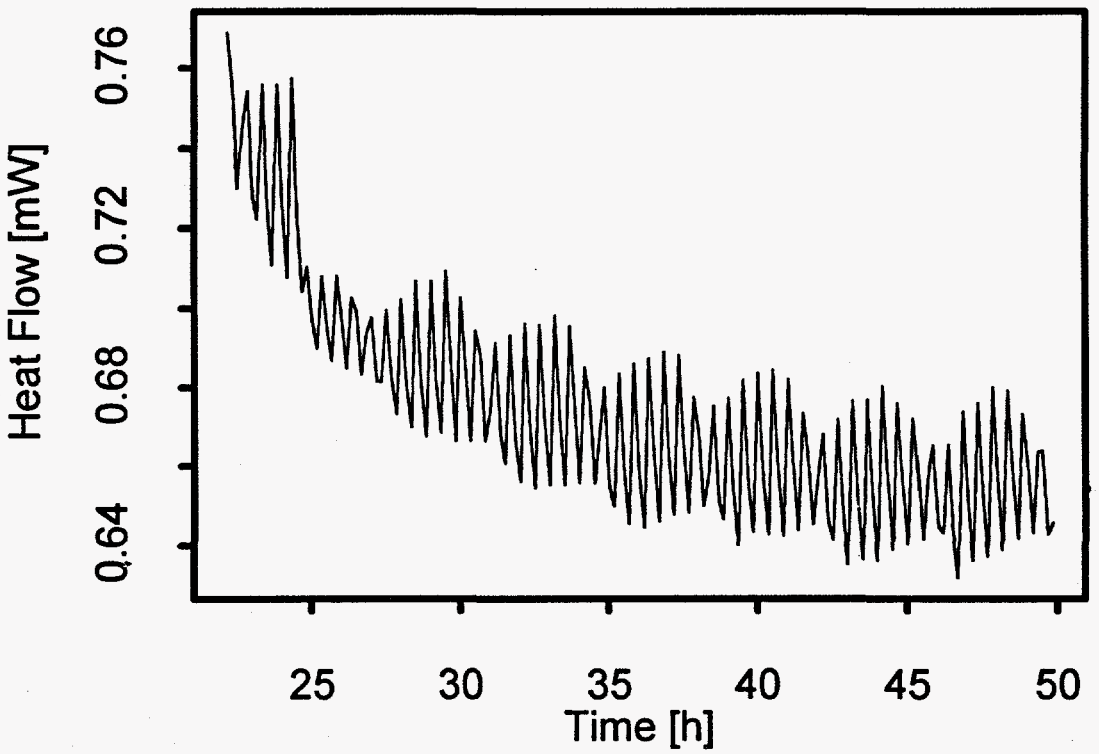

Figure 5: Effect of impedance tests on the heat flow of a Li/TC cell. Each spike is in response to an impedance measurement. The harmonic oscillations are due to asynchronous timing of the heat flow and impedance measurements.

Effects of Direct and Pulsed Current on the Self-Discharge of Li/TC Cells

As discussed above, passage of current enhances the self-discharge of Li/TC cells, apparently because the passivation layer breaks down and allows thionyl chloride to directly react with the lithium anode according to reaction 1. If reactions 1 and 2 proceed completely independent of each other, then any current-induced exposure of lithium metal will bring about a proportional increase of the self-discharge rate and lead to a faradaic efficiency of less than 1. In the absence of such a surface-cleaning current, the cell will still self-discharge in proportion to the area of lithium that is not protected by the lithium chloride layer. Averaged over time, this translates into reduced faradaic efficiency.

Most applications call for uninterrupted use of Li/TC cells, while others require pulse conditions where a comparatively long off-period follows a short period of high current flow. The latter conditions were expected to present the worst possible situation, but as Figure 6 shows, the lowest faradaic efficiency is associated with the lowest average current density. The data in Figure 6 are all based on microcalorimetric determinations of the heat flow from Li/TC cells during DC and pulsed discharge loads. Because of the slow rate at which cells approach steady state conditions, each test was run for a minimum of 3 hours. Apart from controlling the on-off duty cycle and the pulse height of the discharge

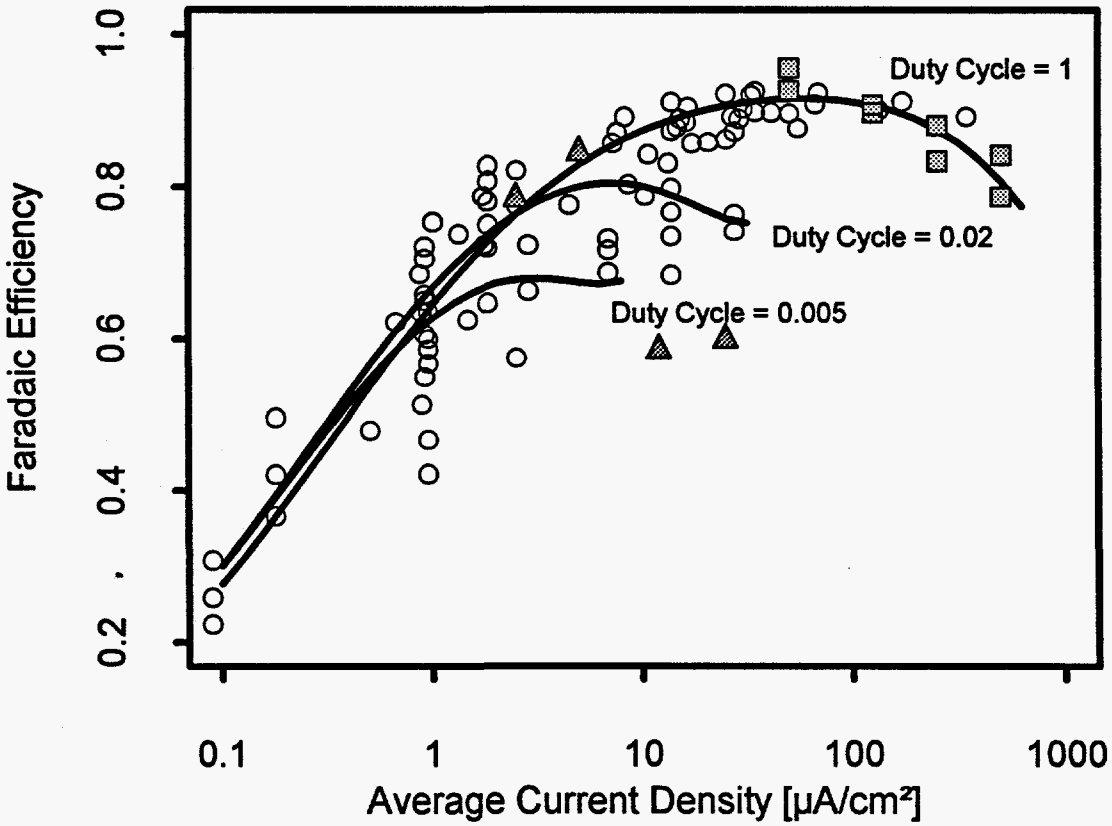

Figure 6: Effect of current density and duty cycle on the faradaic efficiency of Li/TC cells. Squares and triangles refer to DC data from references 4 and 5, respectively.

current, two temperatures, 5 and 30 C, were selected for evaluation, as were cells with different anode areas and different electrolyte concentrations. Using current densities, in lieu of current, eliminates cell size as a factor, but the differences in electrolyte concentration were ignored in the data analysis. Overall, the experiment design is somewhat unbalanced, because it is not practical to test numerous cells with well defined depths of discharge. Expenditures in time and material would have been prohibitive. The slow rate of data acquisition of the microcalorimeter necessitated that each cell be tested under numerous current loads, in order to save time on equipment equilibration. Therefore, if there is an effect of the prior history of a cell it will not be recognized, but the experimental error will be increased. Eight data points in Figure 6 come from P. Bro's paper[4] (squares) and four more from that of Takeuchi et al.[5] (triangles). The former were measured at 25 and 45 C, the latter at 37 C, all with DC. Appendix 1 summarizes the experimental conditions and the measured responses for the SNL data.

The calculation of faradaic efficiencies from microcalorimetric measurements has been discussed in the literature, e.g. by Takeuchi et al.,[5] and involves the separation of several contributions to the total heat output of the cell. In our studies, the cell was placed in the cavity of the calorimeter and connected via thin wires to either a precision resistor (for DC tests) or to an electronic power supply (for pulse measurements). Therefore, all energy from the cell, which could be put to some useful purpose, dissipates outside the calorimeter. Energy dissipation inside the cell derives from three processes, (1) Joule heat due to the voltage drop across the internal cell resistance, (2) entropic heat associated with the anode and cathode reactions, i. e. the Peltier effect, and (3) heat from the self discharge reaction. Item (1) is small and can be neglected, unless the internal resistance is high at very low temperature or has risen to several Ohms as the result of a deep discharge. The entropic heat follows from thermodynamic data for reaction (1)[7,8] and corresponds to about 0.43 T mV (41.3 T Wsec/F), where T is the absolute temperature. Referring this value to the open circuit voltage of 3.65 V yields the ideal heat evolution in the cell as a fraction of the useful energy (3.6% at 30 C). Therefore, if Q_{sd} is the heat due to self discharge, Q_c the calorimetrically measured heat and Q_e the externally dissipated energy, it follows that

$$Q_{sd} = Q_c - 0.43\ T\ Q_e \tag{4}$$

and the faradaic efficiency becomes

$$E_{farad} = 1 - Q_{sd} / Q_e \tag{5}$$

The faradaic efficiency data shown in Figure 6 were subjected to a statistical regression analysis with temperature T_c [C] , current pulse height I_p [$\mu A/cm^2$], duty cycle P, and average current density J [$\mu A/cm^2$] as independent variables. Since efficiencies only vary between zero and one, it is necessary to transform the raw data in order to achieve homogeneity of the system variance. Choosing the Weibull function as a model[9] requires that the regression be carried out consistent with the equation

$$\log(-\log(1-E_{farad}) = f(T, I_p, P, \log(J)) \quad (6)$$

Table 1 shows that the variables log(J) and I_p plus four interactions yield a reasonably good fit to the data, including those taken from Bro's paper. The regression lines shown in Figure 6 were calculated with the coefficients of Table 1, for 30 C and for three levels of the duty cycle P. As seen in the graph, the effect of P disappears as the current density decreases below 1 $\mu A/cm^2$. With regard to temperature, there are statistically significant interactions with pulse height and duty cycle, but its overall effect is small. This result is not inconsistent with the earlier observation that (rapid) temperature changes greatly affect the integrity of the passivation layer and, therefore the rate of self discharge.

Table 1: Multiple Regression Analysis of Faradaic Efficiency Data on a transformed scale according to equation (6)

Residual Standard Error = 0.1485, Multiple R-Square = 0.92
N = 90, F-statistic = 121.8 on 8 and 81 df, p-Value = 0

	Coefficient	Standard Error	t Statistic	p.Value
Intercept	0.1529	0.0366	4.1743	0.0001
I_p	$-8.777\ 10^{-4}$	0.0002	-5.6226	0.0000
log(J)	1.2482	0.0892	13.9955	0.0000
P	-0.6850	0.1548	-4.4248	0.0000
$\log(J)^2$	-0.2312	0.0174	-13.3230	0.0000
$T_c \times \log(J)$	-0.0106	0.0023	-4.5874	0.0000
$T_c \times I_p^2$	$1.126\ 10^{-8}$	0.0000	4.1889	0.0001
$T_c \times I_p^3$	$-1.260\ 10^{-12}$	0.0000	-3.6576	0.0005
$T_c \times P^3$	0.0189	0.0043	4.3855	0.0000

Summary and Conclusion

The efficiency of converting chemical energy into electrical energy has been studied for the case of D-size, low and medium rate lithium-thionyl chloride (Li/TC) cells, under DC and various pulsed loads. Microcalorimetric monitoring of the heat output during discharge allowed the direct measurement of the faradaic efficiency, and showed that self-discharge is far more pervasive than previously acknowledged by researchers and battery manufacturers. Attempts to accelerate the data acquisition by means of impedance tests proved to present an unwarranted risk in view of the fact that the measurements influenced the battery performance.

Evaluations of the cell dynamics prove that current load and temperature fluctuations combine to disrupt the lithium passivation and to greatly enhance self-discharge, as follows:

- Changes in temperature stress the lithium-lithium chloride interface due to differences in the thermal expansion. As a result, the passivation layer cracks and delaminates, which in turn enables the direct contact and spontaneous chemical reaction between lithium and thionyl chloride.
- Current flows wherever the ohmic resistance is lowest., i.e. through cracks and pores in the passivation layer. The anodic reaction, through the removal of lithium, undercuts the LiCl, and thereby enlarges the area of exposed lithium. Starting the discharge with a passivation layer of low porosity may cause the cell voltage to collapse due to minimal current flow, but undercutting of the LiCL will, eventually, remove the constriction. The degree of depassivation depends on the instantaneous current density, with pulsed current exposing more of the lithium surface than DC. Accordingly, pulsed current yields a lower faradaic efficiency than comparable constant current.

Typical faradaic efficiencies for DC range from about 30% at low current density to 90% at moderate and 75 % at high current density. Pulsed current depresses these efficiency levels, except at very low average current densities. The decreased faradaic efficiency of Li/TC batteries in certain pulse situations needs to be studied further to define the range of applications for which it can be successfully used.

References

[1] E. Peled and H. Straze, J. Electrochemical Soc. 127, 1030 (1977).
[2] M. Gaberscek, J. Jamnik and S. Pejovnik, J. Electrochem. Soc. 140, 308 (1993)
[3] M. Kovac, S. Milicev, A. Kovac and S. Pejovnik, J. Electrochem. Soc. 142, 1390 (1995).
[4] P. Bro, Power Sources 7, J. Thompson, Editor, Academic Press, New York (1979)
[5] E. S. Takeuchi, S. M. Meyer and C. F. Holmes, J. Electrochem Soc. 137, 1665 (1990)
[6] F. M. Delnick, IMRA America, Inc. private communication. 1995.
[7] E. S. Takeuchi, J. of Power Sources 24 (1988) 229-241.
[8] N. A. Godshall and J. R. Driscoll, J. Electrochemical Soc. 131, 2221 (1984).
[9] E. T. Eisenmann, "Lithium - Thionyl Chloride Battery State of the Art Assessment," SAND96-0839

Appendix 1: Data Summary

Temperature	On Time[sec]	Off Time[sec]	I_p [mA]	J [$\mu A/cm^2$]	Q_c [mW]	E_{farad}	Q_e [mW]
30	8.	180	0.4	0.0897	0.11	0.308	0.0468
30	2.	180	1.2	0.0897	0.14	0.259	0.0468
30	0.5	180	4.8	0.0897	0.17	0.224	0.0468
30	8.	90	0.4	0.179	0.1	0.495	0.0936
30	2.	90	1.2	0.179	0.135	0.421	0.0936
30	0.5	90	4.8	0.179	0.17	0.366	0.0936
30	86400.	0	0.073	0.503	0.3	0.478	0.263
30	8.	180	3.	0.92	0.261	0.658	0.48
30	2.	180	12.	0.92	0.327	0.606	0.48
30	0.5	180	48.	0.92	0.413	0.549	0.48
30	0.5	180	50.	0.958	0.3	0.636	0.5
5	0.5	180	50.	0.958	0.35	0.599	0.5
30	1.	180	25.	0.958	0.37	0.586	0.5
5	0.5	180	50.	0.958	0.4	0.567	0.5
5	0.5	180	50.	0.958	0.6	0.466	0.5
5	1.	180	25.	0.958	0.72	0.421	0.5
30	36000.	0	0.146	1.01	0.18	0.754	0.526
30	8.	90	3.	1.84	0.283	0.781	0.96
30	2.	90	12.	1.84	0.392	0.719	0.96
30	0.5	90	48.	1.84	0.549	0.647	0.96
30	57600.	0	0.365	2.52	0.3	0.821	1.31
30	57600.	0	0.365	2.52	0.4	0.775	1.31
5	57600.	0	0.365	2.52	1.02	0.574	1.31
5	0.5	60	50.	2.87	0.6	0.724	1.5
5	0.5	60	50.	2.87	0.8	0.663	1.5
30	0.5	50	100.	6.9	1.38	0.732	3.6
30	0.5	100	200.	6.9	1.49	0.716	3.6
30	0.5	200	400.	6.9	1.72	0.687	3.6
30	36000.	0	1.05	7.24	0.664	0.856	3.78
30	36000.	0	1.10	7.59	0.615	0.871	3.96
30	36000.	0	1.20	8.28	0.551	0.891	4.32
30	5.	20	5.	8.62	1.16	0.803	4.5
30	5.	10	3.	10.3	1.53	0.787	5.4
5	36000.	0	2.	13.8	0.74	0.911	7.2
30	36000.	0	2.	13.8	1.1	0.873	7.2
30	5.	5	2.	13.8	1.91	0.798	7.2
30	0.5	50	200.	13.8	2.30	0.766	7.2
30	0.5	100	400.	13.8	2.72	0.735	7.2
30	0.5	200	800.	13.8	3.48	0.684	7.2
30	36000.	0	2.20	15.2	1.04	0.889	7.92
30	36000.	0	2.40	16.6	0.958	0.904	8.64
30	5.	20	10.	17.2	1.58	0.857	9.0
30	5.	10	6.	20.7	1.87	0.858	10.8
5	36000.	0	3.64	25.1	1.17	0.921	13.1
5	36000.	0	3.65	25.2	2.2	0.862	13.1
30	5.	5	4.	27.6	2.21	0.872	14.4
30	0.5	50	400.	27.6	4.66	0.764	14.4

Appendix 1: Data Summary (continued)

Temperature	On Time[sec]	Off Time[sec]	I_p [mA]	J [$\mu A/cm^2$]	Q_c [mW]	E_{farad}	Q_e [mW]
30	0.5	100	800.	27.6	5.26	0.741	14.4
30	36000.	0	4.2	29.	1.99	0.888	15.1
30	36000.	0	4.4	30.3	1.8	0.902	15.8
30	36000.	0	4.8	33.1	1.57	0.920	17.3
5	36000.	0	5.	34.5	1.53	0.925	18.0
30	5.	20	20.	34.5	2.15	0.897	18.0
30	5.	10	12.	41.4	2.59	0.897	21.6
5	36000.	0	7.3	50.3	3.2	0.896	26.3
30	5.	5	8.	55.2	4.25	0.876	28.8
5	36000.	0	10.	69.	3.15	0.923	36.0
5	36000.	0	18.2	126.	7.2	0.905	65.7
5	36000.	0	25.	172.	9.18	0.911	90.0
5	36000.	0	50.	345.	22.9	0.892	180.0
5	0.5	180	110.	0.886	0.662	0.635	1.1
5	0.5	90	110.	1.77	0.88	0.724	2.2
5	2.	180	20.8	0.67	0.53	0.622	0.83
5	2.	90	20.8	1.34	0.62	0.738	1.66
5	6.	180	9.	0.87	0.52	0.685	1.08
5	6.	90	9.	1.74	0.61	0.788	2.16
30	36000.	0	0.6	13.3	0.46	0.831	2.16
30	36000.	0	1.2	26.7	0.55	0.892	4.32
30	36000.	0	3.	66.7	1.15	0.908	10.8
30	36000.	0	6.	133.	2.5	0.900	21.6
30	10.	3590	14.	0.89	0.14	0.512	0.14
30	10.	290	14.	10.7	0.34	0.843	1.74
30	36000.	0	0.73	16.2	0.36	0.884	1.21
30	36000.	0	0.664	14.7	0.35	0.877	1.17
30	36000.	0	0.0664	1.48	0.15	0.625	0.17
30	36000.	0	0.203	4.51	0.22	0.777	0.65
5	0.5	180	48.	0.92	0.27	0.651	0.48
5	0.5	90	48.	1.84	0.335	0.750	0.96
5	2.	180	12.	0.92	0.21	0.705	0.48
5	2.	90	12.	1.84	0.24	0.807	0.96
5	8.	180	3.	0.92	0.195	0.720	0.48
5	8.	90	3.	1.84	0.21	0.827	0.96

Unlimited Release
Initial Distribution

1	MS-0953	W. E. Alzheimer, 1500
1	MS-0613	D. H. Doughty, 1521
1	MS-0614	N. H. Clark, 1522
1	MS-0614	D. E. Mitchell, 1522
1	MS-0614	D. B. Hardy, 1522
1	MS-0614	R. G. Jungst, 1522
1	MS-0614	D. E. Weigand, 1522
1	MS-0614	K. R. Grothaus, 1523
1	MS-0614	N. Doddapaneni, 1523
1	MS-0614	E. T. Eisenmann, 1523
1	MS-0614	R. A. Guidotti, 1523
30	MS-0614	S. N. Hoier, 1523
1	MS-0614	D. Ingersoll, 1523
1	MS-0614	B. Johnson, 1523
1	MS-0614	G. Nagasubramanian, 1523
1	MS-0613	P. C. Butler, 1525
1	MS-0613	J. M. Freese, 1525
1	MS-0613	C. L. Wagner, 1525
1	MS-0340	W. R. Cieslack, 1832
1	MS-0557	W. R. Reynolds, 2103
1	MS-0481	M. M. Harcourt, 2167
1	MS-1072	B. T. Meyer, 2274
1	MS-0557	C. O'Gorman, 2741
1	MS-0557	T. L. Paez, 2741

1	MS-9018	CTF, 8523-2
5	MS-0899	Technical Library, 4414
1	MS-0619	Print Media, 12615
2	MS-0100	Document Processing, 7613-2 for DOE / OSTI